

Vol. 3 • No. 1 • January • 2018

[www.advmattechnol.com](http://www.advmattechnol.com)

# ADVANCED MATERIALS TECHNOLOGIES

WILEY-VCH

# Heterogeneous Integration of Microscale GaN Light-Emitting Diodes and Their Electrical, Optical, and Thermal Characteristics on Flexible Substrates

Lizhu Li, Changbo Liu, Yuanzhe Su, Junchun Bai, Jianqiu Wu, Yanjun Han, Yubin Hou, Shuxian Qi, Yu Zhao, He Ding, Yifei Yan, Lan Yin, Pu Wang, Yi Luo, and Xing Sheng\*

Materials and device strategies to form inorganic, thin-film, microscale light-emitting diodes (micro-LEDs) are presented based on a simplified release method. High performance gallium nitride based blue micro-LEDs are fabricated on and released from both patterned sapphire substrates (PSSs) and conventional nonpatterned sapphire substrates (CSSs). Micro-LEDs are transferred onto copper and polyimide based flexible substrates and their electrical and optical performances are maintained. Thermal properties of PSS and CSS based micro-LEDs are systematically explored on different substrates. Finally, micro-LEDs combined with phosphor coatings demonstrate capability for polychromatic emission. The techniques presented here provide promising paths to advanced light sources with potential applications in lighting, displays, and biomedicine.

Inorganic light-emitting diodes (LEDs) have found numerous applications ranging from general lighting,<sup>[1]</sup> projection, and displays to advanced therapeutics.<sup>[2]</sup> More recently, microscale

L. Li, Dr. C. Liu, Prof. Y. Han, Y. Zhao, Dr. H. Ding,  
Prof. Y. Luo, Prof. X. Sheng  
Department of Electronic Engineering  
Tsinghua National Laboratory for Information Science and Technology (TNList)  
Tsinghua University  
Beijing 100084, China  
E-mail: xingsheng@tsinghua.edu.cn


Y. Su  
Department of Physics  
Tsinghua University  
Beijing 100084, China

J. Bai  
Xi'an Zoomview Optoelectronics Science and Technology Co., LTD  
Xian 710065, China

J. Wu  
FLIR Systems (Shanghai) Co., LTD. Beijing Branch  
Beijing 100004, China

Y. Hou, S. Qi, Prof. P. Wang  
Institute of Laser Engineering  
Beijing University of Technology  
Beijing 100124, China

Y. Yan, Prof. L. Yin  
School of Materials Science and Engineering  
Tsinghua University  
Beijing 100084, China

 The ORCID identification number(s) for the author(s) of this article can be found under <https://doi.org/10.1002/admt.201700239>.

DOI: 10.1002/admt.201700239

LEDs that can be utilized as implantable light sources have been playing increasingly important roles in neuroscience research, along with the development of genetically encoded actuators and indicators.<sup>[3,4]</sup> In particular, gallium nitride (GaN)/indium gallium nitride (InGaN) based blue LEDs are utilized as implantable light sources for optogenetic stimulation and/or exciting fluorophores for neural signal sensing.<sup>[5,6]</sup> High performance GaN blue LEDs are typically grown on rigid, single crystalline substrates including sapphire,<sup>[7,8]</sup> silicon (Si)<sup>[1]</sup> and silicon carbide (SiC),<sup>[9]</sup> and novel strategies on growing and releasing GaN devices on unusual substrates like zinc dioxide coated

graphene,<sup>[10]</sup> boron nitride (BN),<sup>[11]</sup> amorphous glasses,<sup>[12]</sup> nanovoid-mediated substrates,<sup>[13]</sup> etc. are also actively explored.<sup>[14]</sup> Although diced bare LED chips have found their uses in wearable and implantable systems by flip-chip bonding,<sup>[15,16]</sup> thin-film LEDs (with thicknesses less than 10 μm) with various emission wavelengths that are released from original growth substrates and integrated onto flexible and stretchable substrates are more desirable for biomedical applications.<sup>[17]</sup> Recent results have successfully demonstrated that released, thin-film LEDs are integrated with flexible, stretchable, and even biodegradable substrates with better biocompatibilities like improved skin conformance and reduced lesion during implantation.<sup>[5,18,19]</sup> Thin-film, freestanding red and infrared (IR) LEDs based on gallium arsenide can be easily formed by selective sacrificial etching;<sup>[20]</sup> however, conventional techniques for thin-film GaN based purple/blue/green LED release and integration typically rely on sophisticated process steps including laser liftoff (LLO) (for GaN on sapphire),<sup>[21,22]</sup> chemical etching (for GaN on Si),<sup>[1,23,24]</sup> wafer bonding,<sup>[25–27]</sup> layer transfer,<sup>[11]</sup> device pick and place,<sup>[28,29]</sup> etc.,<sup>[30,31]</sup> thus limiting their use. While GaN LED epitaxial liftoff and integration with flexible substrates have been extensively exploited for various planar device architectures like GaN LEDs on graphene,<sup>[7,10]</sup> BN,<sup>[11]</sup> glasses with nanovoids,<sup>[12,13]</sup> Si,<sup>[32]</sup> SiC-on-insulator,<sup>[9]</sup> the performance of these devices is still inferior to their counterparts on conventional sapphire substrates, in terms of their current–voltage characteristics, quantum efficiencies, etc. Therefore, it is highly desirable to develop simple and reliable technologies to implement the mainstream, state-of-the-art GaN LEDs (for example,

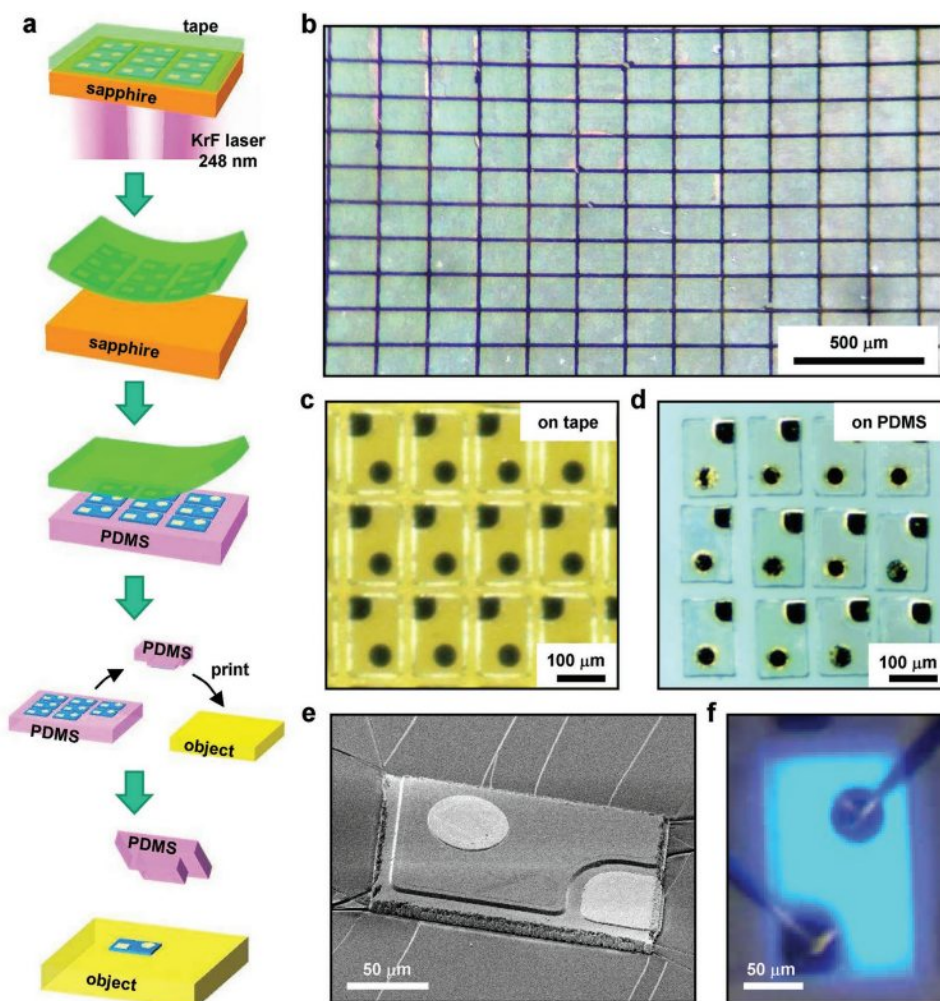


**Figure 1.** a) Schematic illustrations of fabrication steps for releasing thin-film micro-LEDs from sapphire and transferring them onto foreign substrates. b) Optical microscopy image of a large micro-LED array released by LLO and transferred onto a thermal release tape. c) Zoomed-in optical microscopy image of a released micro-LED array on a thermal release tape. d) Optical microscopy image of a released micro-LED array printed on PDMS. e) Scanning electron microscopy (SEM) image (tilted view) of a micro-LED on PDMS. f) Optical microscopy image of a micro-LED with illumination (forward current 1 mA).

LEDs on patterned sapphire substrates, PSSs) for biointegration because of their high performance and ready commercial availability.<sup>[18,33,34]</sup> In addition, thermal management of these heterogeneously integrated LEDs is critically important for biomedical applications, given the fact that typical flexible and stretchable substrates exhibit low thermal conductivities (e.g., only  $\approx 0.12 \text{ W m}^{-1} \text{ K}^{-1}$  for polyimide). In this paper, we present device fabrication and integration concepts to realize micro-scale, thin-film GaN LEDs onto flexible substrates based on a simplified release and transfer process. High performance GaN based micro-LEDs fully formed on both conventional nonpatterned sapphire substrates (CSSs) and PSSs are released and printed onto various flexible substrates including copper (Cu) and polyimide (PI) thin films. We systematically study their structural, electrical, optical, and thermal properties, in comparison with numerical simulations. Integrated with various phosphors, interconnected micro-LED arrays demonstrate the capability of polychromatic emission on curved substrates.

**Figure 1a** schematically illustrates the fabrication flow of forming thin-film, freestanding GaN based micro-LEDs, and their heterogeneous integration onto foreign substrates. The LED structure involves GaN/InGaN multiple quantum wells grown on sapphire substrates (both CSS and PSS) with an emission wavelength centered at around 470 nm. Arrays of LED devices are lithographically patterned and metallized, and released from sapphire by an LLO technique with a krypton fluoride (KrF) excimer laser. By automatically scanning the laser beam, large arrays of micro-LEDs (up to a full 2 inch wafer) can be released with a high yield (>95%), as presented in Figure 1b. Unlike standard LLO process that depends on wafer bonding with rigid substrates,<sup>[24]</sup> here a flexible thermal release tape (TRT) is utilized as a supporting layer to hold the LEDs after LLO. Subsequently, released LEDs are transferred onto a flat polydimethylsiloxane (PDMS) carrier substrate. Later, these freestanding LEDs can be retrieved individually or as arrays by PDMS stamps, and deterministically transferred onto any

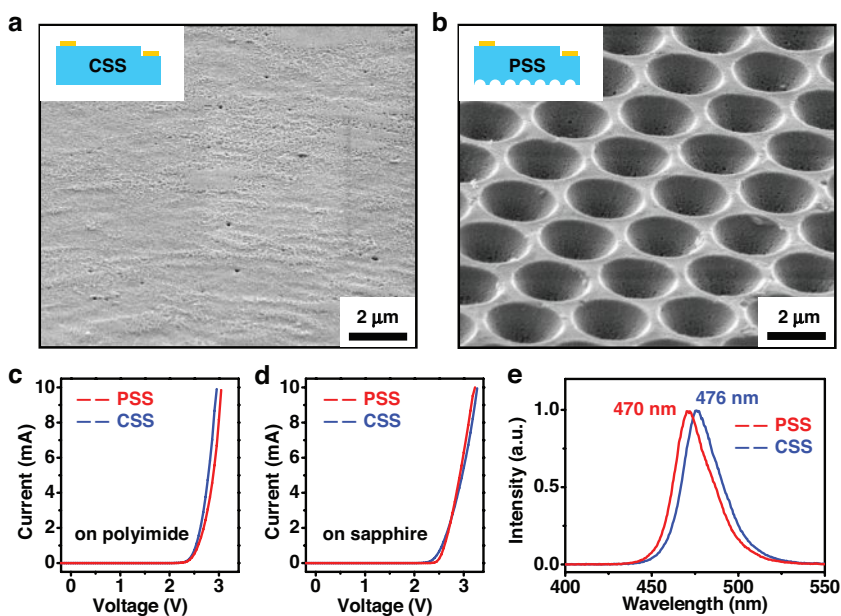


**Figure 2.** a,b) SEM images (tilted view) for the backside surfaces of the micro-LEDs released from CSS a) and PSS b). Insets: schematic illustrations (cross-sectional view) for the micro-LEDs. c) Measured current and voltage characteristics for the micro-LEDs released from CSS and PSS and transferred onto polyimide. d) Measured current and voltage characteristics for the micro-LEDs on original sapphire substrates (CSS and PSS). e) Measured EL spectra for the micro-LEDs from CSS and PSS.

substrates of interest. Figure 1c,d depicts arrays of released micro-LEDs on TRT and PDMS, respectively. The fabricated micro-LED has a dimension of  $180 \times 125 \times 7 \mu\text{m}^3$  (Figure 1e) and can be probed or metallized for current injection (Figure 1f).

The LLO process facilitated with the above TRT-based simplified approach can be implemented for LEDs on both CSS and PSS. Scanning electron microscopic (SEM) images in Figure 2a,b illustrate the backside surfaces (cleaned with ammonia) for LEDs released from CSS and PSS, respectively. The optimized energy densities during LLO are about  $0.6 \text{ J cm}^{-2}$  for CSS and  $0.7 \text{ J cm}^{-2}$  for PSS, which are similar to results reported in literature.<sup>[35]</sup> Captured SEM images of surface morphology clearly reveal that no significant structural damages are associated with the LLO process. Current-voltage characteristics are measured for micro-LEDs released from CSS and PSS and printed onto polyimide, with results shown in Figure 2c. Both LEDs have threshold voltages around 2.5 V and currents reaching  $\approx 10 \text{ mA}$  at 3.0 V, with performance similar to unreleased devices on original sapphire substrates (Figure 2d).

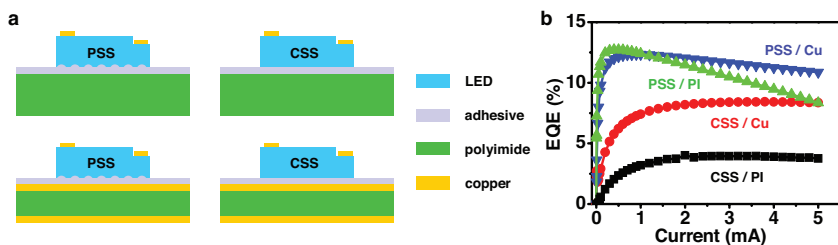


**Figure 3.** a) Schematic illustrations (cross-sectional view) for CSS and PSS micro-LEDs printed on PI and Cu. b) Measured EQE as a function of injected current.

Electroluminescence (EL) spectra for micro-LEDs released from PSS and CSS are measured and plotted in Figure 2e. Though both LEDs are grown under the same experiment condition, the emission peak wavelength of the LED released from PSS (at 470 nm) is slightly shorter than that from CSS (at 476 nm), which is mainly caused by the stress reduction during LED growth on PSS.<sup>[36,37]</sup>

These micro-LEDs released from PSS and CSS can be integrated onto various heterogeneous substrates and their performances have been evaluated. Figure 3a schematically illustrates both types of LEDs transferred onto flexible bare polyimide (PI thickness  $75 \mu\text{m}$ ) and double side Cu coated polyimide ( $18 \mu\text{m Cu}/25 \mu\text{m PI}/18 \mu\text{m Cu}$ ) substrates. A polymer thin-film (thickness  $\approx 1 \mu\text{m}$ )<sup>[38]</sup> serves as an adhesive and electrical insulating layer to bond LEDs and substrates. Figure 3b plot shows the measured external quantum efficiency (EQE) spectra for both types of LEDs on different substrates. For GaN LEDs grown on sapphire, it is generally known that using PSS as growth substrates greatly reduces the stress of the epitaxial layer caused by the mismatch in lattice constant and thermal expansion coefficient,

thus improving both the internal quantum efficiency and light-extraction efficiency.<sup>[39]</sup> Here, we observe that such superior performances are still retained for LEDs that have been released from PSS. Experimentally, the maximum EQE for LEDs from PSS is  $\approx 12\%$ , higher than that for CSS LEDs ( $\approx 8\%$ ). In addition, it can be clearly observed that both LEDs on PI exhibit inferior performance to their counterparts on Cu. This is attributed to the different thermal behaviors of these LEDs, which is to be discussed in detail in Figure 4.

Thermal management is an indispensable topic for consideration during LED operations, since it does not only affect characteristics of LEDs like output power, efficiency, and emission spectrum, but also significantly influences their biocompatibility. For example, temperature rise in brain tissues should be restricted within  $1\text{--}2 \text{ }^\circ\text{C}$  when using implantable LEDs for optogenetic stimulation.<sup>[40]</sup> Micro-LEDs released from PSS and CSS are transfer printed on flexible PI and copper coated polyimide (Cu) substrates, metallized and encapsulated. Subsequently, the flexible PI and Cu substrates are patterned to form needle shapes (width  $\approx 300 \mu\text{m}$ ) by laser milling (Figure 4a). Different currents are injected into micro-LEDs via external power sources, and the temperature distributions on LED needles are imaged using an IR camera. Meanwhile, numerical models based on finite element analysis (FEA) are established to calculate the thermal maps. Figure 4b,c compares experimental and simulated results for micro-LEDs released from CSS and transferred onto Cu and PI substrates, respectively. Under the same injected

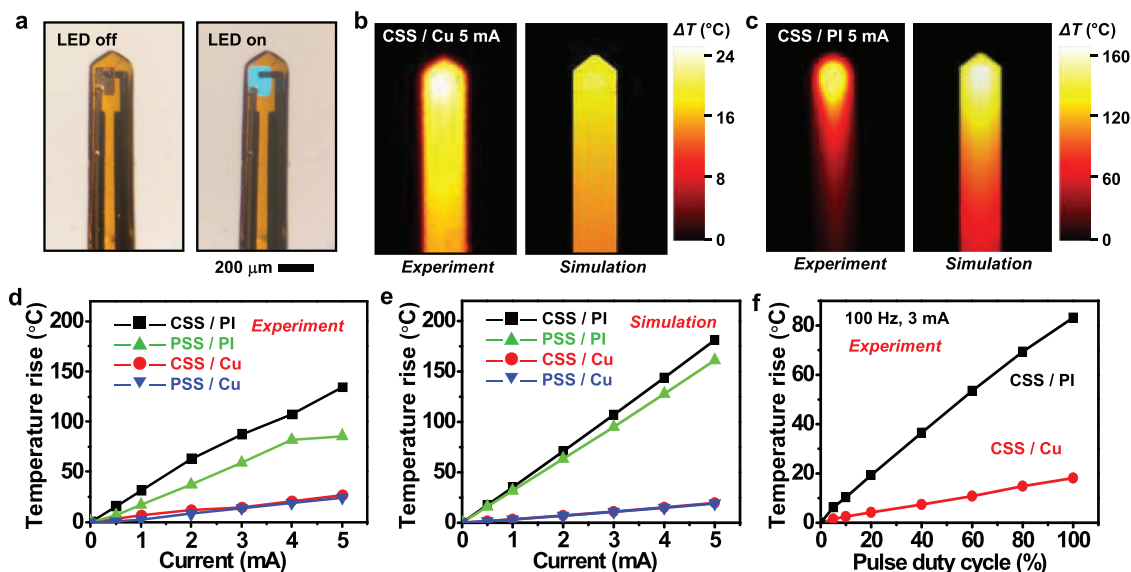


**Figure 4.** a) Microscope images of a micro-LED printed and metallized on a PI-based flexible needle with (right) and without (left) illumination. b,c) Measured (left) and simulated (right) temperature distributions for CSS micro-LEDs on Cu b) and PI c), with an injected current of 5 mA. d) Measured and e) simulated maximum temperature rises (located on the LED surface) as a function of injected current for CSS and PSS micro-LEDs on PI and Cu. f) Measured maximum temperature rises for CSS LEDs on PI and Cu under pulsed current injection (3 mA) with different duty cycles.

current (5 mA), the device printed on Cu exhibits a significantly lower temperature rise ( $\Delta T_{\max} = 24\text{ }^{\circ}\text{C}$ ) than that printed on PI ( $\Delta T_{\max} = 160\text{ }^{\circ}\text{C}$ ), stemming from the difference in thermal conductivities of Cu and PI ( $400\text{ W m}^{-1}\text{ K}^{-1}$  for Cu vs  $0.12\text{ W m}^{-1}\text{ K}^{-1}$  for PI). In addition, the heat is more evenly distributed in Cu than that in PI, also due to the high thermal conductivity of Cu. The experimental results are consistent with numerical simulations, indicating that the FEA model is capable to predict thermal behaviors of micro-LEDs implanted in biological systems that are more challenging to measure directly. Figure 4d,e plots the maximum temperature changes associated with different current injections (under continuous operation) for micro-LEDs released from CSS and PSS and printed on Cu and PI. The experiment and calculation results suggest that the operational temperatures for both LEDs from CSS and PSS can be greatly reduced by introducing a Cu layer between the LED and the PI substrate because of its high thermal conductivity. Moreover, it is noted that the micro-LED released from PSS presents a lower temperature rise than that from CSS (both printed on PI), which is associated with combined

effects of higher quantum efficiency and larger surface area for PSS LEDs. The experimentally measured temperature data in Figure 4d are lower than the simulated results in Figure 4e, particularly at high temperatures ( $\Delta T > 100\text{ }^{\circ}\text{C}$ ). This is mainly because of the inaccuracy of our thermal camera, which is optimized for measuring temperatures below  $150\text{ }^{\circ}\text{C}$ . For some biomedical applications such as optogenetic stimulations in brain tissues, pulsed light output can be employed for neuromodulation,<sup>[41,42]</sup> which can further mitigate thermal effects during LED operation. Figure 4f plots the measured temperature rises for the micro-LEDs released from CSS and printed on Cu and PI. By modulating the duty cycle of pulses, the induced temperature change of LED needles can be reduced, which can be below  $2\text{ }^{\circ}\text{C}$  for the CSS LED on Cu with a pulse duty cycle less than 10% (at a current of 3 mA and a frequency of 100 Hz).

In addition, temperature rises during LED operation cause bandgap narrowing and influence LED emission spectra.<sup>[29]</sup> Figure 5a,b plots normalized emission spectra under various injected currents for micro-LEDs (PSS) on PI and Cu substrates, respectively. For these LEDs, the measured peak

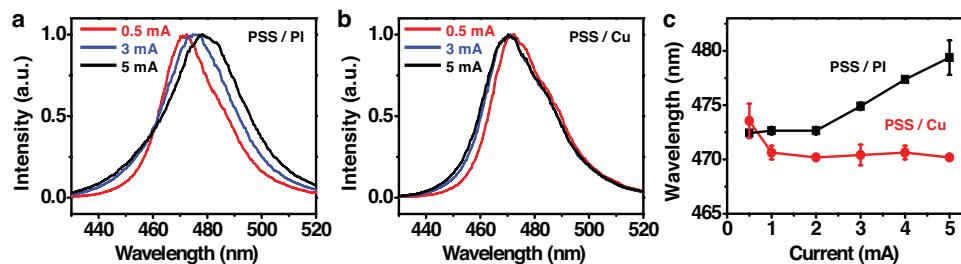


**Figure 5.** a,b) EL spectra for PSS micro-LEDs on PI a) and Cu b) working under different injected currents (0.5, 3, and 5 mA). c) Peak wavelengths of EL spectra for PSS LEDs on PI and Cu as a function of current.

wavelengths as a function of injected current are shown in Figure 5c. Under currents from 0.5 to 5 mA, the micro-LED printed on PI exhibits a peak wavelength shift >5 nm, while no significant spectral shift is observed for the LED on Cu. The spectral measurements are consistent with the thermal behaviors for micro-LEDs (Figure 4).

For some biomedical applications such as optogenetic stimulations, light sources with different emitting wavelengths are required, depending on the specific photoreceptors expressed in neural circuits.<sup>[43]</sup> Although blue light (450–480 nm) is mostly used due to the wide deployment of channelrhodopsin-2, photoreceptors sensitive to other wavelengths are actively studied since they have potential to enable independent optical control of different cell populations. Examples include some recently developed receptors that can be driven by green, yellow, or red lights.<sup>[44]</sup> To realize these emission wavelengths, one can exploit other III–V semiconductor based LEDs (e.g., InGaN, gallium phosphide (GaP), aluminum indium gallium phosphide (AlInGaP), etc.),<sup>[45]</sup> but challenges including low efficiency of green/yellow semiconductor emitters and the difficulty related to hybrid device integration remain daunting. Another feasible approach is to integrate downshifting phosphors with specific emission colors onto blue InGaN LEDs.<sup>[19]</sup> Advantages of using phosphors include high quantum yields, low cost, and the ease for implementation. For demonstration, phosphors with different colors (green, yellow, and red) are mixed into PDMS and coated on the surface of micro-LED needles. **Figure 6a–d** illustrates their emission spectra and corresponding optical photographs. By selecting appropriate phosphors, the peak wavelengths of emission can be adjusted from 470 nm (bare GaN blue LED) to 525 nm (green), 558 nm (yellow), and 628 nm (red), respectively. Under an injected current of 1 mA, the light output power density on the surface of these LED needles is estimated to be larger than  $10 \text{ mW mm}^{-2}$ , which is well above the required light energy (typically  $1\text{--}5 \text{ mW mm}^{-2}$ ) to activate the corresponding photoreceptors.<sup>[42]</sup>

These epitaxially released micro-LEDs can be transfer printed onto flexible substrates and interconnected deterministically to form light-emitting arrays. A flexible array including five micro-LEDs connected in parallel is formed (Figure 6e). Polyimide (75 nm thick) serves as the supporting substrate for the interconnected LED array, which is patterned by laser milling and attached to a thin sheet of PDMS. Current and voltage characteristics are almost invariant when the array is deformed (with a bending radius of 1 cm). In addition, no significant

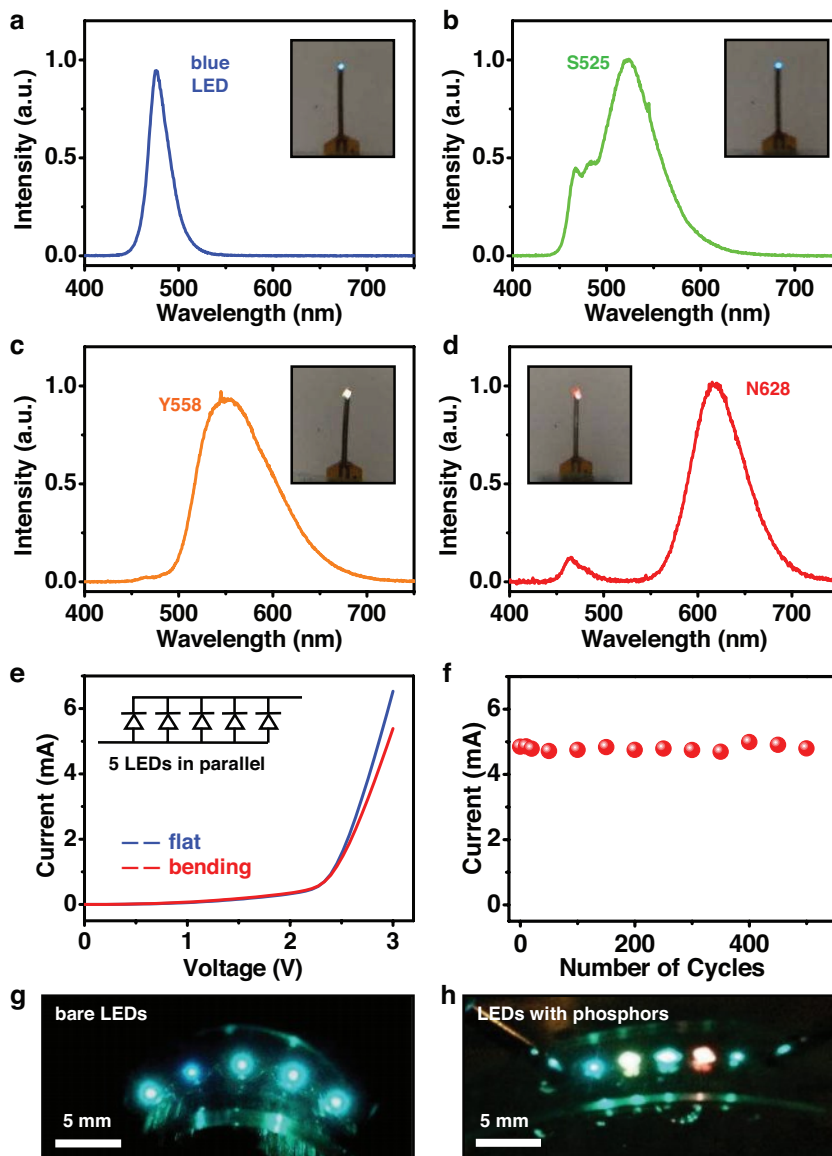


**Figure 6.** a–d) EL spectra for micro-LEDs coated with different phosphors: a) bare LED, b) LED with S525 (green), c) LED with Y558 (yellow), and d) LED with N628 (red). Insets show the microscopic images for micro-LEDs with different illumination colors. e) Current and voltage characteristics of an array with five micro-LEDs in parallel with and without bending deformation. Inset shows the LED circuit diagram. f) Measured current of the micro-LED array at a voltage of 3 V during 500 cycles of bending deformation. g, h) Photographs of the deformed LED array without g) and with h) phosphor coatings wrapped on a curved PDMS substrate with a bending radius of about 1 cm.

performance degradation is observed after 500 cycles of bending (Figure 6f). Figure 6g illustrates the uniform light emission for these five parallel connected micro-LEDs under bending condition. Furthermore, the photograph of LEDs coated with different phosphors (Figure 6h) demonstrates their polychromatic emission capability.

In summary, this paper discusses a simplified fabrication approach to effectively form thin-film microscale GaN based blue LEDs and deterministically integrated them with heterogeneous substrates. Released from PSS and CSS, micro-LEDs on PI and Cu substrates are comprehensively investigated in

terms of their electrical, optical, and thermal properties. With further size reduction, active arrays of such blue micro-LEDs can be utilized to form flexible, efficient, and high brightness displays by combining with phosphors or other III–V based emitters.<sup>[46]</sup> Integrated onto thin-film needle substrates, the micro-LEDs can find their immediate use as injectable light sources for deep brain optogenetic stimulations.<sup>[47]</sup> Combined with wireless power delivery techniques, micro-LED arrays on flexible and biocompatible substrates also have potentials to serve as wearable or implantable emitters for optical sensors and light therapy.<sup>[16]</sup> The results presented here provide viable routes to the development of advanced light sources for versatile applications in lighting, displays, and biomedicine.

## Experimental Section

**Fabrication of Micro-LEDs:** The GaN based LED structures were grown on 2 inch sapphire substrates (PSS and CSS) using metal-organic chemical vapor deposition. The PSS pattern had a pitch of 3  $\mu\text{m}$ , a width of 2  $\mu\text{m}$ , and a height of 1  $\mu\text{m}$ . The LED structure (from bottom) included the sapphire substrate, a GaN buffer layer, an n-GaN, an InGaN/GaN multiple-quantum-well layer, and a p-GaN. The thickness of the entire epitaxial structure was about 7.1  $\mu\text{m}$ . LED devices were lithographically fabricated, with Ohmic contacts made by sputtered layers of 100 nm indium tin oxide/10 nm chrome (Cr)/ 100 nm gold (Au) for p-GaN and 10 nm Cr/100 nm Au for n-GaN. The LED mesa (lateral dimension 180  $\times$  125  $\text{mm}^2$ ) was defined by inductively coupled plasma (ICP) reactive ion etching, with 4 mTorr pressure, 40 sccm  $\text{Cl}_2$ , 5 sccm  $\text{BCl}_3$ , 5 sccm Ar, ICP power 450 W, bias power 75 W, and an etch rate of 0.33  $\mu\text{m min}^{-1}$ . After bonding the fully fabricated LED arrays onto a TRT (Nitto Denko Corp.), LLO was applied to separate the thin-film LEDs from sapphire substrates by thermally decompose GaN into gallium (Ga) metal and nitrogen gas at the interface. A KrF excimer laser at 248 nm (Coherent, Inc., CompexPro110) served as the light source, with a uniform illumination area of 5 mm  $\times$  15 mm. The laser beam was automatically scanned across LED wafers. The power density during LLO was optimized to be around 0.6 and 0.7  $\text{J cm}^{-2}$  for LEDs on CSS and PSS, respectively. After laser irradiation, the micro-LEDs were released from sapphire by mild mechanical force at 70  $^\circ\text{C}$  (the melting point of Ga is 29.7  $^\circ\text{C}$ ). The Ga residual was removed by immersing the samples into dilute ammonia (1:10 in water) at room temperature. By heating up to 120  $^\circ\text{C}$ , the LEDs were detached from the TRT (the critical release temperature is about 110  $^\circ\text{C}$ ). Released LEDs were bonded onto patterned PDMS substrates and then were picked up individually or in arrays using flat PDMS stamps and transferred onto other substrates. The key to successful retrieval lied in the difference of adhesion forces between patterned and flat PDMS.<sup>[20]</sup>

**LED Transfer Printing:** The released freestanding LEDs were transferred onto any substrates, with a spin-coated adhesive layer.<sup>[38]</sup> The LEDs printed onto polyimide (75  $\mu\text{m}$ ) or double side copper coated polyimide (18  $\mu\text{m}$  Cu/25  $\mu\text{m}$  PI/18  $\mu\text{m}$  Cu) substrates (with 1  $\mu\text{m}$  thick SU-8 for adhesion) were encapsulated with 2  $\mu\text{m}$  thick SU-8 as an insulating layer and via patterns were formed by interconnected electrodes with sputtered 10 nm Cr/600 nm Cu/100 nm Au. UV laser milling was applied to form the shape of the LED needle or flexible circuits. Different phosphors (S525 for green, YAG558 for yellow, and N628 for red) were mixed with PDMS (1:10 weight ratio) and casted on the LEDs (thickness 100  $\mu\text{m}$ ) for polychromatic emission.

**Device Characterization:** The current–voltage relation was measured by a source meter (Keithley 2400) under illumination. The EQE and output power measurements were performed using an integrating sphere (Labsphere Inc.) and an Si photodetector. The thermal images were acquired by an IR camera (FLIR A655sc) with a close-up lens (25  $\mu\text{m}$ ). The IR camera was calibrated using a hot plate with standard digital temperature indicators. It should be noted that the IR camera

presented some inaccuracies for measuring high temperatures >150  $^\circ\text{C}$ . LED emission spectra were collected with a spectrometer (Ocean Optics HR2000+).

**Thermal Modeling:** 3D steady-state heat transfer models were built via a finite element analysis model (Comsol Multiphysics). The model accounted for the heat transfer through different substrates (Cu or PI), as well as the natural heat convection to air. The LED served as the heat source, with the input thermal power estimated by  $P = V \times I \times (1 - \text{EQE})$ , where  $V$  and  $I$  are the measured voltage and current for LEDs.

## Acknowledgements

L.L. and C.L. contributed equally to this work. Y.S. and Y.Y. acknowledge the support from Tsinghua Student Research Training (SRT) Program. L.Y. and X.S. acknowledge the support from National Natural Science Foundation of China (NSFC Projects 51602172 and 51601103) and 1000 Youth Talents Program in China. X.S. also acknowledges support from Science and Technology Innovation Commission of Shenzhen (JCYJ20170411140807570). Y.H. and Y.L. acknowledge National Basic Research Program of China (Grant No. 2015CB351900).

## Conflict of Interest

The authors declare no conflict of interest.

## Keywords

flexible devices, indium gallium nitride, laser liftoff, microscale LEDs, transfer printing

Received: September 5, 2017

Revised: October 3, 2017

Published online: November 22, 2017

- [1] H.-S. Kim, E. Brueckner, J. Song, Y. Li, S. Kim, C. Lu, J. Sulkin, K. Choquette, Y. Huang, R. G. Nuzzo, J. A. Rogers, *Proc. Natl. Acad. Sci. USA* **2011**, *108*, 10072.
- [2] S. H. Yun, S. J. Kwok, *Nat. Biomed. Eng.* **2017**, *1*, 0008.
- [3] T. Knöpfel, *Nat. Rev. Neurosci.* **2012**, *13*, 687.
- [4] J. Akerboom, N. C. Calderón, L. Tian, S. Wabnig, M. Prigge, J. Tolö, A. Gordus, M. B. Orger, K. E. Severi, J. J. Macklin, R. Patel, S. R. Pulver, T. J. Wardill, E. Fischer, C. Schluer, T. W. Chen, K. S. Sarkisyan, J. S. Marvin, C. I. Bargmann, D. S. Kim, S. Kügler, L. Langnado, P. Hegemann, A. Gottschalk, E. R. Schreier, L. L. Looger, *Front. Mol. Neurosci.* **2013**, *6*, 2.
- [5] S. I. Park, D. S. Brenner, G. Shin, C. D. Morgan, B. A. Copits, H. U. Chung, M. Y. Pullen, K. N. Noh, S. Davidson, S. J. Oh, J. Yoon, K.-I. Jang, V. K. Saminen, M. Norman, J. G. Grajales-Reyes, S. K. Vogt, S. S. Sundaram, K. M. Wilson, J. S. Ha, R. Xu, T. Pan, T.-I. Kim, Y. Huang, M. C. Montana, J. P. Golden, M. R. Bruchas, R. W. Gereau, J. A. Rogers, *Nat. Biotechnol.* **2015**, *33*, 1280.
- [6] R. Scharf, T. Tsunematsu, N. McAlinden, M. D. Dawson, S. Sakata, K. Mathieson, *Sci. Rep.* **2016**, *6*, 28381.
- [7] W.-S. Choi, H. J. Park, S.-H. Park, T. Jeong, *IEEE Photonics Technol. Lett.* **2014**, *26*, 2115.
- [8] Y. Jung, X. Wang, J. Kim, S. H. Kim, F. Ren, S. J. Pearton, J. Kim, *Appl. Phys. Lett.* **2012**, *100*, 231113.
- [9] C.-H. Cheng, T.-W. Huang, C.-L. Wu, M. K. Chen, C. H. Chu, Y.-R. Wu, M.-H. Shih, C.-K. Lee, H.-C. Kuo, D. P. Tsai, G. R. Lin, J. *Mat. Chem. C* **2017**, *5*, 607.

- [10] K. Chung, C.-H. Lee, G. C. Yi, *Science* **2010**, *330*, 655.
- [11] Y. Kobayashi, K. Kumakura, T. Akasaka, T. Makimoto, *Nature* **2012**, *484*, 223.
- [12] J. H. Choi, A. Zoukarneev, I. K. Sun, W. B. Chan, H. Y. Min, S. S. Park, H. Suh, U. J. Kim, H. B. Son, J. S. Lee, M. Kim, J. M. Kim, K. Kim, *Nat. Photonics* **2011**, *5*, 763.
- [13] J. H. Choi, E. H. Cho, S. L. Yun, M.-B. Shim, H. Y. Ahn, C.-W. Baik, E. H. Lee, K. Kim, T.-H. Kim, S. Kim, K.-S. Cho, J. Yoon, M. Kim, S. Hwang, *Adv. Opt. Mater.* **2014**, *2*, 267.
- [14] J. H. Choi, J. Kim, H. Yoo, J. Liu, S. Kim, C. W. Baik, C. R. Cho, J. G. Kang, M. Kim, P. V. Braun, S. Hwang, T.-S. Jung, *Adv. Opt. Mater.* **2016**, *4*, 505.
- [15] J. Kim, A. Banks, Z. Xie, S. Y. Heo, P. Gutruf, J. W. Lee, S. Xu, K.-I. Jang, F. Liu, G. Brown, J. Choi, J. H. Kim, X. Feng, Y. Huang, U. Paik, J. A. Rogers, *Adv. Funct. Mater.* **2015**, *25*, 4761.
- [16] J. Kim, G. A. Salvatore, H. Araki, A. M. Chiarelli, Z. Xie, A. Banks, X. Sheng, Y. Liu, J. W. Lee, K. I. Jang, S. Y. Heo, K. Cho, H. Luo, B. Zimmerman, J. Kim, L. Yna, X. Feng, S. Xu, M. Fabiani, G. Gratton, Y. Huang, U. Paik, J. A. Rogers, *Sci. Adv.* **2016**, *2*, e1600418.
- [17] T.-I. Kim, R.-H. Kim, J. A. Rogers, *IEEE Photonics J.* **2012**, *4*, 607.
- [18] C. Goßler, C. Bierbrauer, R. Moser, M. Kunzer, K. Holc, W. Pletschen, K. Köhler, J. Wagner, M. Schwaerzle, P. Ruther, O. Paul, J. Neef, D. Keppeler, G. Hoch, T. Moser, U. T. Schwarz, *J. Phys. D: Appl. Phys.* **2014**, *47*, 205401.
- [19] G. Shin, A. M. Gomez, R. Al-Hasani, Y. R. Jeong, J. Kim, Z. Xie, A. Banks, S. M. Lee, S. Y. Han, C. J. Yoo, J. L. Lee, S. H. Lee, J. Kurniawan, J. Tureb, Z. Guo, J. Yoon, S. I. Park, S. Y. Bang, Y. Nam, M. C. Walicki, V. K. Samineneni, A. D. Mickle, K. Lee, S. Y. Heo, J. G. McCall, T. Pan, L. Wang, X. Feng, T. I. Kim, J. K. Kim, Y. Li, Y. Huang, R. W. Gereau IV, J. S. Ha, M. R. Bruchas, J. A. Rogers, *Neuron* **2017**, *93*, 509.
- [20] S.-I. Park, Y. Xiong, R.-H. Kim, P. Elvikis, M. Meitl, D.-H. Kim, J. Wu, J. Yoon, C.-J. Yu, Z. Liu, Y. Huang, K.-C. Hwang, P. Ferreira, X. Li, K. Choquette, J. A. Rogers, *Science* **2009**, *325*, 977.
- [21] Y. S. Wu, J.-H. Cheng, W. C. Peng, H. Ouyang, *Appl. Phys. Lett.* **2007**, *90*, 251110.
- [22] W. Chen, X. N. Kang, X. D. Hu, R. Lee, Y. J. Wang, T. J. Yu, Z. J. Yang, G. Y. Zhang, L. Shan, K. X. Liu, X. D. Shan, L. P. You, D. P. Yu, *Appl. Phys. Lett.* **2007**, *91*, 121114.
- [23] H. G. Yoo, K.-I. Park, M. Koo, S. Kim, S. Y. Lee, S. H. Lee, K. J. Lee, *Proc. SPIE* **2012**, *8268*, 82681Y-1.
- [24] T.-I. Kim, Y. H. Jung, J. Song, D. Kim, Y. Li, H.-S. Kim, I.-S. Song, J. J. Wierer, H. A. Pao, Y. Huang, J. A. Rogers, *Small* **2012**, *8*, 1643.
- [25] S. C. Hsu, C. Y. Liu, *Electrochem. Solid-State Lett.* **2006**, *9*, G171.
- [26] S.-C. Hsu, D. S. Wu, C.-Y. Lee, J. Y. Su, R.-H. Horng, *IEEE Photonics Technol. Lett.* **2007**, *19*, 492.
- [27] B. Ji, M. Wang, X. Kang, X. Gu, C. Li, B. Yang, X. Wang, J. Liu, *IEEE Trans. Electron Devices* **2017**, *64*, 2008.
- [28] J.-H. Seo, J. Li, J. Lee, S. Gong, J. Lin, H. Jiang, Z. Ma, *IEEE Photonics J.* **2015**, *7*, 1.
- [29] T.-I. Kim, S. H. Lee, Y. Li, Y. Shi, G. Shin, S. D. Lee, Y. Huang, J. A. Rogers, J. S. Yu, *Appl. Phys. Lett.* **2014**, *104*, 051901.
- [30] H.-Y. Kuo, S.-J. Wang, P.-R. Wang, K.-M. Uang, T.-M. Chen, S.-L. Chen, W.-C. Lee, H.-K. Hsu, J.-C. Chou, C.-H. Wu, *IEEE Photonics Technol. Lett.* **2008**, *20*, 523.
- [31] W.-S. Choi, W. J. Kim, S.-H. Park, S. O. Cho, J. K. Lee, J. B. Park, J.-S. Ha, T. H. Chung, T. Jeong, *Solid-State Electron.* **2017**, *127*, 57.
- [32] H.-S. Kim, E. Brueckner, J. Song, Y. Li, S. Kim, C. Lu, J. Sulkin, K. Choquette, Y. Huang, R. G. Nuzzo, J. A. Rogers, *Proc. Natl. Acad. Sci. USA* **2011**, *108*, 10072.
- [33] T.-M. Chang, H. K. Fang, C. Liao, W.-Y. Hsu, Y. S. Wu, *ECS J. Solid State Sci. Technol.* **2015**, *4*, R20.
- [34] J. Chun, Y. Hwang, Y.-S. Choi, J.-J. Kim, T. Jeong, J. H. Baek, H. C. Ko, S.-J. Park, *Scr. Mater.* **2014**, *77*, 13.
- [35] J.-H. Lee, J.-T. Oh, S.-B. Choi, Y.-C. Kim, H.-I. Cho, J.-H. Lee, *IEEE Photonics Technol. Lett.* **2008**, *20*, 345.
- [36] T. S. Oh, H. Jeong, Y. S. Lee, T. H. Seo, A. H. Park, H. Kim, K. J. Lee, M. S. Jeong, E. K. Suh, *Thin Solid Films* **2011**, *519*, 2398.
- [37] J. H. Lee, J. T. Oh, J. S. Park, J. W. Kim, Y. C. Kim, J. W. Lee, H. K. Cho, *Phys. Status Solidi* **2006**, *3*, 2169.
- [38] T.-I. Kim, M. J. Kim, Y. H. Jung, H. Jang, C. Dagdeviren, H. A. Pao, S. J. Cho, A. Carlson, K. J. Yu, A. Ameen, H. J. Chung, S. H. Jin, Z. Ma, J. A. Rogers, *Chem. Mater.* **2014**, *26*, 3502.
- [39] G. Yang, J. Chang, J. Zhao, Y. Tong, F. Xie, J. Wang, Q. Zhang, H. Huang, D. Yan, *Mater. Sci. Semicond. Process.* **2015**, *33*, 149.
- [40] M. E. Llewellyn, K. R. Thompson, K. Deisseroth, S. L. Delp, *Nat. Med.* **2010**, *16*, 1161.
- [41] F. Zhang, A. M. Aravanis, A. Adamantidis, L. de Lecea, K. Deisseroth, *Nat. Rev. Neurosci.* **2007**, *8*, 577.
- [42] E. S. Boyden, F. Zhang, E. Bamberg, G. Nagel, K. Deisseroth, *Nat. Neurosci.* **2005**, *8*, 1263.
- [43] F. Zhang, L. Wang, M. Brauner, J. F. Liewald, K. Kay, N. Watzke, P. G. Wood, E. Bamberg, G. Nagel, A. Gottschalk, K. Deisseroth, *Nature* **2007**, *446*, 633.
- [44] N. C. Klapoetke, Y. Murata, S. S. Kim, S. R. Pulver, A. Birdsey-Benson, Y. K. Cho, T. K. Morimoto, A. S. Chuong, E. J. Carpenter, Z. Tian, J. Wang, Y. Xie, Z. Yan, Y. Zhang, B. Y. Chow, B. Surek, M. Melkonian, V. Jayaraman, M. Constantine-Paton, G. K. S. Wong, E. S. Boyden, *Nat. Methods* **2014**, *11*, 338.
- [45] E. F. Schubert, T. Gessmann, J. K. Kim, *Light Emitting Diodes*. 2nd ed., Cambridge University Press, New York, USA **2006**.
- [46] C. A. Bower, M. A. Meitl, B. Raymond, E. Radauscher, R. Cok, S. Bonafede, D. Gomez, T. Moore, C. Prevatte, B. Fisher, B. Fisher, R. Rotzoll, G. A. Melnik, A. Fecioru, A. J. Trindade, *Photonics Res.* **2017**, *5*, A23.
- [47] T.-I. Kim, J. G. McCall, Y. H. Jung, X. Huang, E. R. Siuda, Y. Li, J. Song, Y. M. Song, H. A. Pao, R.-H. Kim, C. Lu, S. Dan Lee, I. S. Song, G. Shin, R. Al-Hasani, S. Kim, M. P. Tan, Y. Huang, F. G. Omenetto, J. A. Rogers, M. R. Bruchas, *Science* **2013**, *340*, 211.